INTERNATIONAL JOURNAL OF AGRICULTURE & BIOLOGY
ISSN Print: 1560–8530; ISSN Online: 1814–9596
18–0441/2019/21–2–391–398
DOI: 10.17957/IJAB/15.0000
http://www.fspublishers.org

Full Length Article

Phenotypic Response of Tobacco Leaves to Simulated Acid Rain and its Impact on Photosynthesis

Yue Wang, Xiu-li Zhang, Yan-bo Hu, Zhi-yuan Teng, Shu-bo Zhang, Qi Chi and Guang-yu Sun*
College of Life Science, Northeast Forest University, Harbin Heilongjiang, 150040, P R China
*For correspondence: sungy@vip.sina.com; 2807866840@qq.com

Abstract

As the number of urban vehicles in China continues to increase rapidly, acid rain from nitrogen wet deposition is becoming progressively more serious. This increases the local importance of breeding and screening for plant varieties resistant to acid rain. In the present study, we investigated the responses of leaf phenotype, net photosynthetic rate, and photosystem II (PSII) to wet deposition of acid rain (simulated by a mixture of sulfuric and nitric acid, at pH values of 3.5, 4.5 and 5.5) on leaves of tobacco seedlings grown in greenhouse conditions. The results showed that leaves sprayed with pH 3.5 acid rain lose green pigmentation and develop yellow spots as well as decrease in net photosynthetic rate. PSII responded to the acid rain treatment with obvious increases in energy flux trapped per reaction center (TR_o/RC), dissipation of energy flux per cross section (DI_o/RC), and the absorbed energy flux per reaction center (ABS/RC). However, there were decreases in photosynthetic performance index (PI_{ABS}), the accumulation of PSII receptor side Q_A^- (V_J), the Q_A maximum rate (M_o), and the heterogeneity of the PQ library (V_I). It suggested that the wet deposition of simulated acid rain in tobacco leaves decreased the stability of thylakoid membranes, inhibited the electron transfer on the donor side and the receptor side of PSII, and destroyed the photosynthetic apparatus. © 2019 Friends Science Publishers

Keywords: Acid rain; Morphology; Gas exchange; Chlorophyll a fluorescence; Photosystem II

Introduction

Acid rain generally refers to any form of precipitation with pH less than 5.6. Acid rain is mainly caused by an artificial emission of acidic substances, such as nitrogen dioxide and sulfur dioxide, into the atmosphere. Therefore, acid rain can harm the plant, aquatic plant and animals, destroy the balance of the terrestrial ecosystem. Accordingly, many governments have made efforts to control and mitigate SO_2 emissions and to change energy production methods. In China, nitrogen oxides (NO_x) in the city is about 1/3 from the emission of fixed sources (steel, cement, electricity, etc.), and 2/3 comes from the emission of motor vehicles (Wang *et al*., 2012). However, NO_x emissions have increased evidently because of the rapidly increase in the number of motor vehicles, thus increasing the relative contribution of nitrate ion (NO_3^-) to acidification. This has substantially decreased the ratio between atmospheric SO_4^{2-} and NO_3^-, resulting in acid rain gradually shifting from sulfuric acid toward nitric acid in composition (Tu *et al*., 2005; Lv *et al*., 2014). Acid rain has negative impacts on forests, bodies of fresh water, and soils as well as human health. Plants, as the dominant component of terrestrial ecosystems, have become the main receptor of acid rain pollution. Accordingly, acid rain effects on plant growth have been examined in different plant species.

First, acid rain affects the morphological structure of plants. It can cause leaf injuries, consist of chlorotic mottling, marginal necrosis, and cuticular damage (Bussotti *et al*., 1997; Shan *et al*., 1997; Hou and Yi, 2000). Adams *et al*. (1984) reported that acid rain first damaged the leaf surface, eventually affecting the internal tissues in the following order: leaf surface waxy layer, epidermal cells, palisade cells, stomata, and the chloroplast lamellar structure. Second, acid rain has several effects on the physiology and biochemistry of plants. Seedling growth is a key impact of acid rain. Early plant growth becomes restricted, mainly as a result of stress toxicity, accompanying with an imbalance of nutrient uptake, and a buildup of toxic ions (Hoorn *et al*., 2001; Neves *et al*., 2009; Dias *et al*., 2010). Nitrogen metabolism and nuclei acid metabolism are also impacted in plant leaves. Acid rain will disturb nitrogen metabolism in plants through a down-regulation of the key enzymes such as nitrate reductase (NR), and glutamine syntheses (GS). Soluble protein content and free amino acid content in the leaves also declined with the acid rain pH (Solomonson and Spehar, 1977). The metabolism of nutrients in plants is also affected. Owing to the increase in sulfate and nitrate ion concentration on acid rain, the activity of hydrogen ions is increased, which expedites the exchange of hydrogen ions with cations in plant cells. Moreover, the stratum cornea and

To cite this paper: Wang, Y., X.L. Zhang, Y. Hu, Z.Y. Teng, S.B. Zhang, Q. Chi and G.Y. Sun, 2019. Phenotypic response of tobacco leaves to simulated acid rain and its impact on photosynthesis. *Intl. J. Agric. Biol*., 21: 391–398

the surface cells of the leaves are harmed by the action of acid rain, increasing the permeability of cells. The combined effect of these two aspects leads to high levels of leaching of plant nutrient ions (Smith, 1990). More broadly, plant photosynthesis is impacted. Normally, exposure to abiotic stresses, to some extent, commonly leads to an inhibition of cellular activity and damage to photosynthetic membranes, correspondingly a decline in leaf photosynthesis (Sheng *et al*., 2008).

Overall, acid rain damages plants by increasing the membrane permeability of leaves, decreasing the activity of membrane protective enzymes, disrupting the metabolic balance of the plant reactive oxygen species, aggravating membrane lipid peroxidation, and generally affecting plant photosynthesis, respiration, nitrogen metabolism and nutrition metabolism. Among these effects, the significant reduction of the photosynthetic rate is one of the most important features. Assimilatory power (NADPH and ATP), an accompanying component in plant photosynthesis, depends on the proton gradient across thylakoid membranes. Moreover, proton gradients are an vital element in the photosynthetic apparatus, permitting the conversion from solar to chemical energy. The extent to which acid rain affects the light reaction in photosynthesis is unclear as well as whether it affects photosystem I (PSI) or photosystem II (PSII). We used tobacco as an experimental system for investigating these issues. Specifically, fluorescence kinetics was used to determine the changes in proton formation and changes in the thylakoid membrane during the process of electron transfer, in combination with assays of morphological changes. This was conducted to identify the sites at which PSII are impacted by acid rain and the degree of this effect.

Materials and Methods

Experimental Materials and Treatments

Experiments were conducted at the Plant Physiology Laboratory of Northeast Forestry University (NEFU), Harbin, China. Tobacco seeds were sown on January 1, 2017. When the seedlings grown to 15 cm in height, these were individually transplanted into pots measuring 16 cm in diameter and 20 cm in height, filled with a 2:1 (*v*/*v*) mixture of coconut soil and vermiculite. When the seedlings reached the four-leaf stage, 30-cm tobacco plants with consistent growth were selected for the acid rain treatments.

The acid rain solution was prepared as described by Hou and Yi (2000) using a solution of 1 m Mol (H_2SO_4) L^{-1} and 1 m Mol (HNO_3) L^{-1} at a chemical equivalent ratio of 5:1. The main salt ion concentrations of the preparation of the electrolyte stock solution were 31.46 mg • L^{-1} NaF, 26.28 mg • L^{-1} KCl, 74.91 mg • L^{-1} $CaCl_2$, 171.28 mg • L^{-1} $MgSO_4$, and 82.27 mg • L^{-1} NH_4Cl. This stock solution was diluted 1000-fold, yielding solutions with pH values of 3.5, 4.5, and 5.5 for use as acid rain test solutions. The solutions were calibrated with a pHS-2C pH meter (Jiangsu Zhengji Instruments Co., Ltd., Jiangsu, China), and water was used as the control (CK). The prepared test solutions were stored in labeled brown glass reagent bottles. Acid rain (500 mL) was sprayed onto plants once each day between 7:00 and 8:00 A.M. for a week. Each time, plants were sprayed with fine droplets from the blade tip downward. To prevent contamination between treatments, plants undergoing different treatments were separated with plastic film.

Methods of Measurement

Determination of electrolyte leakage rate: The fresh leaves of plants were punched into 80–100 round pieces of material, which rinsed with deionized water three times, dried, mixed, and set aside. Then, 20 punched leaf samples were placed into each 15-mL test tube, with 3 per treatment group, depressed to the bottom of each tube with a clean glass rod, and covered in 10 mL of deionized water. Test tubes were then placed into a dryer, which was pumped for 10 min with a vacuum pump to extract any air in the cellular gaps of the material; the deflated plant material then sank to the bottom of the test tubes. After 20 min at room temperature, the conductivity of the leaf wafer extract and a deionized water control sample was determined using a conductivity meter. Test tubes were then measured after 15-min incubation in a boiling water bath at 100°C to kill plant cells. After cooling the samples in tap water for 10 min, the conductivity, *i.e.*, electrolyte exudation rate, was measured using the following formula: electrolyte leakage rate = (sample conductivity - blank conductivity) / (boiled sample conductivity - blank conductivity) × 100%.

Determination of Thiobarbituric Acid Reactive Substances Content

Thiobarbituric acid reactive substances (TBARS) content was determined colorimetrically using thiobarbituric acid according to the method described by Buege *et al.* (1987). First, 1 g of chopped material was added to 2 mL of 10% trichloroacetic acid (TCA) and a small amount of quartz sand and ground into a homogenate; 8 mL of TCA was added before further grinding, followed by centrifugation of the homogenate at 4000 r/min for 10 min and extraction of the supernatant from the sample. After the supernatant of the centrifuged sample was removed, the remaining 2 mL sample (for the control, 2 mL of distilled water was used instead) was added to 2 mL of 0.6% thiobarbituric acid (TBA) solution. The mixture was placed in a boiling water bath for 15 min, quickly cooled, and then centrifuged again. The supernatant was used to measure the absorbance at wavelengths of 532, 600, and 450 nm. The malondialdehyde (MDA) contents was calculated according to formula $C = 6.45 (A_{532} - A_{600}) - 0.56A_{450}$, $y = (C \bullet V) / W$,

where *C* is the concentration of TBARS, *A* is the absorbance value; *V* is the volume of the extract, *W* is the fresh weight of plant tissue, and *y* is the TBARS content.

Determination of Superoxide Anion Content

Superoxide anion content was determined using the kit produced by Suzhou Keming Company (Suzhou, China) for determination. The determination principle was: the reaction of superoxide anion with hydroxylamine hydrochloride produces NO_2^-, NO_2^- generates a red azo compound under the action of p-aminobenzenesulfonic and α-naphthylamine and has a characteristic absorption at 530 nm, which O_2^- content in the sample can be calculated from the A_{530} value, the reaction equation is $NH_2OH+2O_2^-+H^+ \rightarrow NO_2^- +H_2O_2+H_2O$.

Determination of Chlorophyll Content

Chlorophyll content was assayed for each plant by extracting 0.25 g of plant tissue with 10 mL of 96% (*v*/*v*) ethanol. Chlorophyll *a* and *b* concentrations were calculated according to the method used by Lichtenthaler and Wellburn (1983).

Determination of Gas Exchange Parameters

Gas exchange parameters were determined by a portable photosynthetic system (LI-COR Biosciences, Lincoln, NE, USA). The measurements were performed under the conditions: a photosynthetic photon flux density (PPFD) of 1000 μmol $m^{-2}\cdot s^{-1}$, concentration of CO_2 of 385 ± 5 $cm^3\cdot m^{-3}$ and temperature of 28 ± 2ºC. Measurements were conducted from 8:30–12:30 on cloudless days.

Fast Chlorophyll Fluorescence Induction Kinetics Curves Determination

After a 0.5-h dark adaptation period of the leaves, the OJIP curve was induced by pulsed light of 3500 μmol $m^{-2}\cdot s^{-1}$ and assayed using a palm chlorophyll fluorescence meter (FluorPen FP 100 max, Photon Systems Instruments, Drásov, Czech Republic). The fourth (from the top) mature expanded leaf of each plant was selected for measurement, and the specific measurement sites on each leaf were between the third and fourth veins of the leaf base, about 2 cm from the main veins. The OJIP curves were plotted using the measured relative fluorescence values, where the O, J, I and P points on the curve are expressed as the corresponding points of the curve at times 0, 2, 30 and 1000 ms, respectively. The L point is 0.15 ms on the corresponding point, while the K point represents the corresponding point on the curve at 0.3 ms. The OJIP curve is based on previous research by Strasser (1997) developed for the purpose of conducting JIP-test analyses. The difference between the normalized O-P of the treated and control plants (CK), respectively, is denoted as $\triangle V_{O\text{-}P}$. In addition, the chlorophyll fluorescence parameters were analyzed: PSII maximum photochemical efficiency (F_v/F_m), primary light energy conversion efficiency (F_v/F_o), PSII potential activity (F_m/F_o), photosynthetic performance index (PI_{ABS}), the accumulation of PSII receptor side Q_A^- (V_J), the reduction of the Q_A maximum rate (M_o), absorption light energy per reaction center (*ABS*/*RC*), trapped light energy for reducing Q_A per reaction center (TR_o/RC), trapped light energy for electron transport per reaction center (ET_o/RC), dissipated light energy per reaction center (DI_o/RC), maximum quantum yield of non-photochemical quenching (ΦD_o), absorption of light available for Q_A after the electron transport chain quantum yield (ΦE_o), and the heterogeneity of the PQ library (V_I). Each indicator was measured three times.

Data Processing and Statistical Analysis

The averages with standard deviations (SDs) were calculated using the Microsoft Office Excel Statistical Package (Microsoft Office, 2013); the significance of difference between treatments was analyzed by one-way ANOVA and tested by the *t*-test with a significance level of 5% ($P < 0.05$) or 1% ($P < 0.01$).

Results

Acid rain Effects on Leaf Injuries

The different simulated acid rain pH treatments were associated with different degrees of leaf damage. The observed symptoms were mainly yellow-brown and dark brown discolored patches between margins and veins as well as curled leaves and overall shrinkage. In our experiments, pH 5.5 acid rain caused no visible damage to treated leaves. However, pH 4.5 acid rain caused slight damaged, with some leaves exhibiting a loss of green pigmentation in spots, and pH 3.5 acid rain caused more severe leaf damage, in which the leaves began to produce local, scattered dark red and necrotic spots of about 0.2 cm in diameter, affecting about 20% of the total leaf area (Fig. 1a, b, c and d).

Effects on Electrolyte Leakage Rate, Thiobarbituric Acid Reactive Substances Content, Superoxide Anion Production Rate and Chlorophyll Content

After acid rain treatment, the electrolyte leakage rate and thiobarbituric acid reactive substances content of the leaves increased relative to the control plants. This suggests that acid rain increases membrane peroxidation and thus membrane permeability. Compared with the control, electrolyte leakage rate and thiobarbituric acid reactive substances content increased by 21.00% ($P > 0.05$) and 187.25% ($P > 0.05$), respectively, at pH; 5.5; 127.71%

Fig. 1: Effect of simulated acid rain on visible leaf damage in leaves of tobacco seedlings

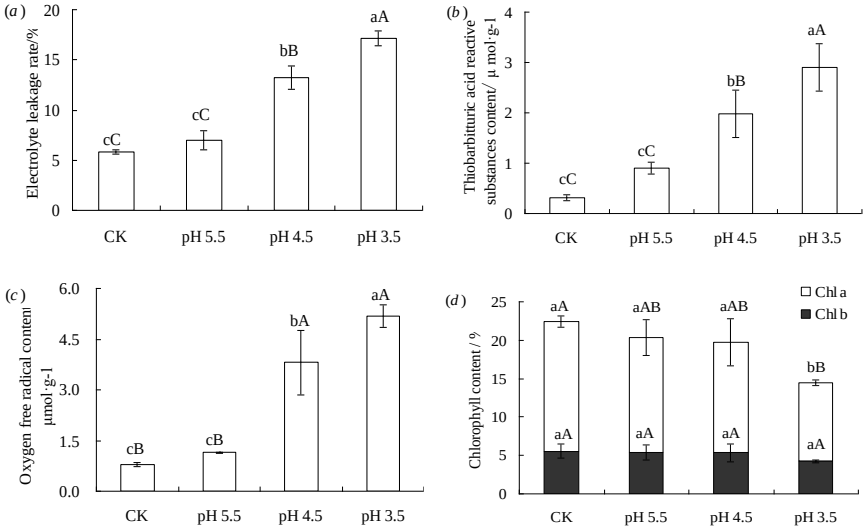

Fig. 2: Effects of simulated acid rain on physiological parameters in leaves of tobacco seedlings
Note: Different lower cases and capital letters for the same parameter mean significant difference among different treatments at 0.05 and 0.01 level, respectively

($P < 0.01$) and 532.93% ($P < 0.01$), respectively, at pH 4.5; 194.66% ($P < 0.01$) and 831.26% ($P < 0.01$), respectively at pH 3.5 (Fig. 2a and b).

As the pH of acid rain decreased, the generation rate of superoxide (SOD) anions increased, with increases of 46% ($P > 0.05$), 385% ($P < 0.01$), and 561% ($P < 0.01$) at pH 5.5, pH 4.5 and pH 3.5, respectively (Fig. 2c).

Chlorophyll *a* content was more sensitive than chlorophyll *b* to the effects of simulated acid rain treatment. The reductions in chlorophyll *a* were 12% ($P > 0.05$), 15% ($P > 0.05$) and 40% ($P < 0.01$) at pH 5.5, pH 4.5, and pH 3.5, respectively. However, there was no significant difference in chlorophyll *b* between different pH treatments and the control treatment ($P > 0.05$; Fig. 2d).

Effect of Acid Rain on Gas Exchange Parameters

In this experiment, the net photosynthetic rate (P_n), stomatal conductance (G_s), and transpiration rate (T_r) under simulated acid rain treatments were lower than the control. P_n, G_s, and T_r were decreased by 20% ($P < 0.05$), 19% ($P < 0.05$), and 30% ($P < 0.01$), respectively, at pH 5.5; 28% ($P < 0.01$), 56% ($P < 0.01$), and 60% ($P < 0.01$), respectively, at pH 4.5; and 51% ($P < 0.01$), 77% ($P < 0.01$), and 80% ($P < 0.01$), respectively, at pH 3.5 (Fig. 3a, b and c). The intercellular CO_2 concentration (C_i) was higher than control, by 118% ($P < 0.01$) and 191% ($P < 0.01$), pH 4.5 and pH 3.5, respectively, while C_i was 58% ($P > 0.05$) of the control value at pH 5.5 (Fig. 3d).

Effects of Acid Rain on OJIP Curve

Acid rain changed the shape of the fast chlorophyll fluorescence induction kinetics curves (OJIP) curve in tobacco leaves (Fig. 4a), and the relative fluorescence intensities F_o, F_J, F_I, and F_P of points O, J, I and P were higher than control. Comparisons of the effects of different simulated acid rain treatments on the variable fluorescence intensity at each point of the OJIP curve revealed the following relative differences between the control and experimental treatments for points O, J, I and P, respectively: 80.74% ($P < 0.01$), 96.15% ($P < 0.01$), 79.95% ($P < 0.01$), and 48.68% ($P < 0.01$) at pH 5.5; 102.72% ($P < 0.01$), 101.10% ($P < 0.01$), 76.32% ($P < 0.01$) and 31.76% ($P < 0.01$) at pH 4.5; and 95.07% ($P < 0.01$), 73.04% ($P < 0.01$), 46.01% ($P < 0.01$), and 20.36% ($P < 0.05$) at pH 3.5 (Fig. 4b). The OJIP curve of the leaves was normalized by O-P,

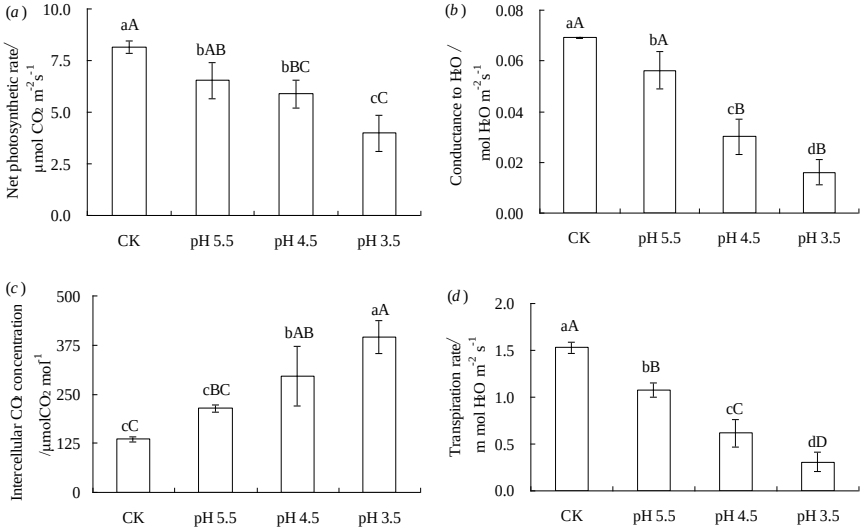

Fig. 3: Effect of simulated acid rain on photosynthetic characteristics in leaves of tobacco seedlings

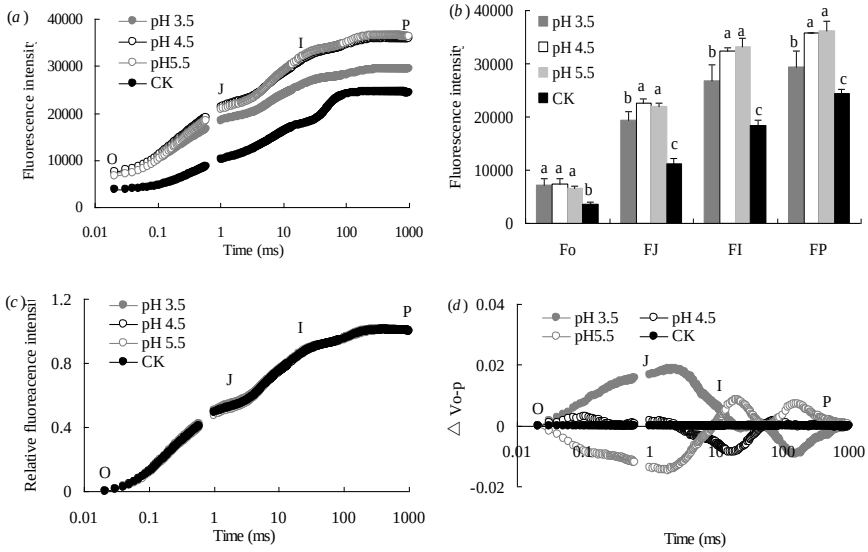

Fig. 4: Effects of simulated acid rain on the O-P curve in leaves of tobacco seedlings

revealing that the relative variable fluorescence of J point of the OJIP curve of the simulated acid rain treatment was significantly increased (Fig. 4c). The difference between the control and acid rain treatments for this measure was greatest at a pH of 3.5 and the difference between $\triangle V_t$ and the control was the most significant at 2 ms (J point) (Fig. 4d).

Effects of Acid Rain on Chlorophyll *a* Fluorescence Parameters

The light absorption based on the photosynthetic system performance index (PI_{ABS}), primary photochemical efficiency (F_v/F_o), the maximum photochemical efficiency (F_v/F_m) and PSII potential activity (F_m/F_o) were lower than control plants, at relative levels of 71.82% ($P < 0.01$), 26.03% ($P < 0.01$), 5.26% ($P > 0.05$), and 21.93% ($P < 0.01$), respectively at pH 5.5; 77.75% ($P < 0.01$), 36.62% ($P < 0.01$), 8.58% ($P < 0.05$), and 30.86% ($P < 0.01$), respectively, at pH 4.5; and 83.62% ($P < 0.01$), 47.31% ($P < 0.01$), 13.13% ($P < 0.01$), and 39.84% ($P < 0.01$), respectively, at pH 3.5 (Fig. 5).

The relative variable fluorescence intensity (V_J) and (V_I) of points J (2 ms) and I (20 ms) on the OJIP curve and the maximum rate (M_o) for Q_A reduction can be used to analyze the redox state of the PSII electron ;transport chain receptor side, and these variables exhibited the following relative values compared to the control: 41.79% ($P < 0.01$), 25.97% ($P < 0.01$), and 92.53% ($P < 0.01$), respectively, at pH 5.5; 45.75% ($P < 0.01$), 24.60% ($P < 0.01$) and 98.00% ($P < 0.01$), respectively, at pH 4.5; 50.75% ($P < 0.01$), 25.07% ($P < 0.01$), and 107.52% ($P < 0.01$), respectively, at

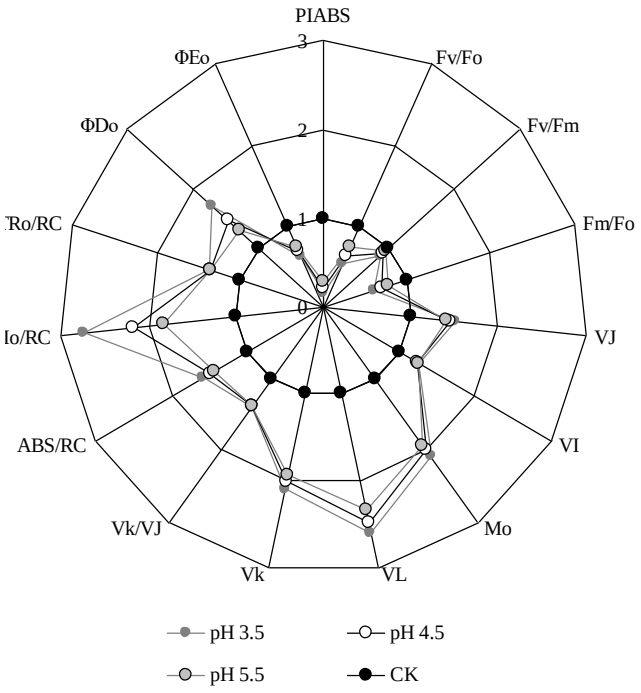

Fig. 5: Effects of simulated acid rain on chlorophyll a fluorescence parameters in leaves of tobacco seedlings

pH 3.5.

The relative variable fluorescence intensities (V_L) and (V_K) of points L (0.15 ms) and K (0.3 ms) on the OJIP curve and the ratio V_K/V_J can be used to analyze thylakoid membrane stability and the activity of the oxygen evolving complex (OEC).

Under the acid rain treatments, V_L, V_K and V_K/V_J generally increased, exhibiting values relative to the control treatment of 133.94% ($P < 0.01$), 93.52% ($P < 0.01$) and 36.48% ($P < 0.01$), respectively, at pH 5.5; 148.72% ($P < 0.01$), 100.06% ($P < 0.01$) and 37.25% ($P < 0.01$), respectively, at pH 4.5; and 159.06% ($P < 0.01$), 109.01% ($P < 0.01$) and 38.64% ($P < 0.01$), respectively, at pH 3.5.

After acid rain treatment, the absorption light energy per reaction center (*ABS*/*RC*), the dissipated light energy per reaction center (DI_o/RC), and the light energy reducing Q_A per reaction center (TR_o/RC) were higher than those of control, with relative differences of 43.25% ($P < 0.01$), 83.57% ($P < 0.01$), and 35.75% ($P < 0.01$), respectively, at pH 5.5; 48.75% ($P < 0.01$), 118.31% ($P < 0.05$) and 35.75% ($P < 0.01$), respectively, at pH 4.5; 59.08% ($P < 0.01$), 174.58% ($P < 0.01$), and 37.50% ($P < 0.01$), respectively, at pH 3.5.

The maximum quantum yield of non-photochemical quenching (ΦD_o) after treatments was higher than the control by 28.12% ($P > 0.05$), 45.88% ($P < 0.05$) and 70.19% ($P < 0.01$) at pH 5.5, pH 4.5 and pH 3.5, respectively. The absorption of light available for Q_A after the electron transport chain quantum yield (ΦE_o) was lower than control by 26.87% ($P < 0.01$), 31.46% ($P < 0.01$), and 37.21% ($P < 0.01$) at pH 5.5, pH 4.5, and pH 3.5, respectively.

Discussion

Tobacco leaves treated with mixed simulated acid rain (pH ≤ 4.5) for 7 days exhibited visible damage, which became more serious as the pH of the acid rain decreased. The leaf damage was the most serious when impacted by acid rain at pH of 3.5, with symptoms of the affected leaves showing irregular yellowish brown and dark brown patches between the leaf margin and veins, curled leaves, overall shrinkage, difficulty in expansion, spots with diameters of about 0.2 cm, and overall affected areas accounting for about 20% of the total leaf area. This result with tobacco was similar to Zhao *et al.* (2010) with *Camellia sasanqua*. The lower pH of the acid rain is associated generally with chlorophyll degradation, chlorophyll content decreases, and/or leaf tissue necrosis (Fan and Wang, 2000; Shaukat and Khan, 2008; Verma *et al*., 2010).

Many experimental studies have shown that simulated acid rain treatments affect photosynthesis in plants, resulting in a decrease in the net photosynthetic rate of plant leaves (Mai *et al*., 2008; Chastain *et al*., 2014; Tong and Zhang, 2014). The stomata are the channel through which CO_2, water vapor, and other gaseous substances enter and exit plant tissues. Plants often adapt to environmental changes or stress conditions by opening and closing stomata. Stomatal conductance is an important index for measuring the degree of stomatal openings. The change in the transpiration rate affects the utilization of water conditions to some extent, reflecting the capacity of plants to adapt to environmental conditions (Zhao *et al*., 2010). At pH 3.5 simulated acid rain treatment, the net photosynthetic rate (P_n), stomatal conductance (G_s), and transpiration rate (T_r) were reduced, but the intercellular CO_2 concentration (C_i) was significantly increased. These four parameters are affected by many environmental factors, as well as negative and positive interactions among those factors. Acid rain reduction or inhibition of plant photosynthesis is the result of a variety of factors, including both osmotic stress-induced stomatal limiting factors and non-stomatal limiting factors such as CO_2 assimilation (Cakmak and Marschner, 1992; Eegineer *et al*., 2016). When the intercellular CO_2 concentration and stomatal conductance are reduced, the stomatal factors are the main factors (Eegineer *et al*., 2016). When the intercellular CO_2 concentration increases, but stomatal conductance decreases, the non-stomatal factors are the main factors (Cakmak and Marschner, 1992). Accordingly, in the present experiments, the net photosynthetic rate decreased, and non-stomatal factors were the main factors. When plant leaves are subjected to acid rain stress, the stomatal conductance decreases, the photosynthetic activity of mesophyll cells also decreases resultings in a decrease in the net photosynthesis rate, which reduced the depletion of intercellular CO_2, thus increasing the

CO_2 concentration in the cells (Gabara *et al*., 2003).

PSII is the most sensitive component of the plant photosynthetic apparatus with respect to environmental stress. Changes in the chlorophyll fluorescence kinetics parameter reflect the influence of the external environment on plants to some extent (Mcgegor *et al*., 2003; Kalaji *et al*., 2016); thus, it can be used as an index of stress damage to plants (Krause and Weis, 1991; Jiang *et al*., 2003; Hu *et al*., 2015). The change in the chlorophyll fluorescence rapid induction kinetic curve (*i.e*., OJIP curve) reflects the photochemical status of PSII (Synkova *et al*., 1998). In this experiment, wet deposition of simulated acid rain changed the shape of the OJIP curve, thus indicating that PSII structure and function were affected by acid rain stress. The photosynthetic system performance index PI_{ABS} reflects the original photochemical quantum yield and can also reflect the density of the reaction center and the transmission of electrons between PSI and PSII. Additionally, based on light energy capture, absorption and electron transport reflects the activity of the light system, with sensitivity greater than the maximum photochemical efficiency F_v/F_m (Zivcak *et al*., 2008). Therefore, PI_{ABS} was used as the effective fluorescence parameter for the response of tobacco to acid rain. In this experiment, the PI_{ABS} of the simulated acid rain-treated leaves was significantly lower than control, which indicated that the simulated acid rain treatment inhibited the electron transport of PSII. Under the acid rain treatments, the energy absorbed by the reaction center (*ABS*/*RC*), the energy consumed by the reaction center (DI_o/RC), and the energy used to restore the Q_A in the reaction center (TR_o/RC) were significantly higher than in the control. Using these parameters, this experiment demonstrated that acid rain stress may reduce the activity of the reaction center or lead to the inactivation of part of the reaction center. The OJIP curve was impacted at points K and L under the acid rain treatment. This effect on point K and the ratio V_K/V_J raised suggests that the oxygenation complex (OEC) was severely damaged, while the impact on point L indicates that the stability of the thylakoid membrane decreased and the donor side of PSII within the electron transfer was inhibited (Strasser, 1997). The accumulation of PSII receptor side Q_A^- (V_J), the reduction of the Q_A maximum rate (M_o), and the heterogeneity of the PQ library (V_I) were significantly decreased in treated plants compared with the control plants, which indicated that the electron transport of the PSII receptor was affected by simulated acid rain (Govindjee, 1995; Strasser *et al*., 1995; Zhang *et al*., 2018). The cause of PSII electrons being blocked on the donor side may have been the high concentration of HSO_3^- and SO_3^{2-} in the cells being converted into SO_3^{2-} in the chloroplast, thus reducing the activity of the OEC. This, in turn, would have decreased the stability of the thylakoid membrane, affecting PSII electron transfer (Lee *et al*., 2001). Accordingly, some stress to plants may cause reversible inactivation of the PSII reaction center. Inactivation of the reaction center make it act as an energy trap that absorbs light but is unable to pass the electrons to the next level of the electron transport chain. Inactive reaction centers can be restored to activity by various adaptive mechanisms (Strasser *et al*., 2004). Under normal circumstances, the PSII reaction center captures light energy, then transferred to the next level, with the remaining energy consumed in the form of heat. In this study, the absorption of light energy per reaction center (*ABS*/*RC*), dissipation of light energy per reaction center (DI_o/RC), and trapped light energy for reducing Q_A per reaction center (TR_o/RC) were significantly higher in the experimental plants than the control plants, indicating that the leaf reaction center activity was affected by simulated acid rain stress. Additionally, the maximum quantum yield of non-photochemical quenching (ΦD_o) increased as acid rain pH decreased, while the absorption of light available for Q_A after the electron transport chain quantum yield (ΦE_o) decreased gradually, indicating that the reaction center was absorbing excess energy, mainly used for non-photochemical quenching.

Conclusion

Under acid rain stress, leaves lose green pigmentation and develop yellow spots. The electrolyte leakage rate, the thiobarbituric acid reactive substances content and superoxide anion production rate in leaves of the tobacco increased. The PSII photochemical activities of the leaves were significantly inhibited. The reason for the decreased PSII photochemical activity of the tobacco leaves sprayed with acid rain was mainly related to the obstruction of electron transfer on the donor side and the receptor side of PSII, and destroyed the photosynthetic apparatus.

Acknowledgments

This work was funded by the National Natural Science Foundation of China (31870373) and the Major Project for Heilongjiang Province Science and Technology Program (GZ13B004).

References

Adams, C.M., N.G. Dengler and T.C. Hutchinson, 1984. Acid rain effects on foliar histology of *Artemisia tilesii*. *Can. J. Bot*., 62: 463–474

Buege, J., S. Aust and J.A. Bueqe, 1987. Aust SD microsomal lipid peroxidation. *Meth. Enzymol*., 52: 302–310

Bussotti, F., A. Bottacci, P. Grossoni and C. Tani, 1997. Cytological and structural changes in Pinus pines L. needles following the application of an anionic surfactant. *Plant Cell Environ*., 20: 513–520

Cakmak, I. and H. Marschner, 1992. Magnesium deficiency and high light intensity enhance activities of superoxide dismutase, ascorbate peroxidase, and glutathione reductase in bean leaves. *Plant Physiol*., 98: 1222–1227

Chastain, D.R., J.L. Snider, G.D. Collins, C.D. Perry, J. Whitaker and S.A. Byrd, 2014. Water deficit in field-grown Gossypium hirsutum primarily limits net photosynthesis by decreasing stomatal conductance, increasing photorespiration, and increasing the ratio of dark respiration to gross photosynthesis. *J. Plant Physiol*., 171: 1576–1585

Dias, B.B., M.D.L. Leite, P.V. Farago, A.V.D. Oliveira and G.C. Beruski, 2010. Sulfur effect by simulated acid rain on morphophysiological parameters of the bean plant. *Acta Sci.-Agron*., 32: 433–439

Eegineer, C.B., M. Hashimotosugimoto, J. Negi, M. Israelssonnordstrom, T. Azoulayshemer, W. Rappel and K. Iba, 2016. CO_2 Sensing and CO_2 Regulation of stomatal conductance: advances and open questions. *Trends Plant Sci*., 21: 16–30

Fan, H.B. and Y.H. Wang, 2000. Effects of simulated acid rain on germination, foliar damage, chlorophyll contents and seedling growth of five hardwood species growing in China. *For. Ecol. Manage*., 126: 321–329

Gabara, B., M. Sklodowska, A. Wyrwicka, S. Glinska and M. Gapinska, 2003. Changes in the ultrastructure of chloroplasts and mitochondria and antioxidant enzyme activity in *Lycopersicon esculentum* Mill. leaves sprayed with acid rain. *Plant Sci*., 164: 507–516

Govindjee, 1995. Sixty-three years since Kautsky: Chlorophyll a fluorescence. *Aust. J. Plant Physiol*., 22: 131–160

Hoorn, J.W.V., N. Katerji, A. Hamdy and M. Mastrorilli, 2001. Effect of salinity on yield and nitrogen uptake of four grain legumes and on biological nitrogen contribution from the soil. *Agric. Water Manage*., 51: 87–98

Hou, B.F. and H.W. Yi, 2000. Effects of simulated acid rain on germination, foliar damage, chlorophyll contents and seedling growth of five hardwood species growing in China. *For. Ecol. Manage*., 126: 321–329

Hu, J., X. Huang, L. Chen and Z. Jianru, 2015. Site-specific nitrosoproteomic identification of endogenously S-nitrosylated proteins in *Arabidopsis*. *Plant Physiol*., 167: 1731–1746

Jiang, C.D., H.Y. Gao and Q. Zou, 2003. Changes of donor and acceptor side in photosystem 2 complex induced by iron deficiency in attached soybean and maize leaves. *Photosynthesis*, 41: 267–271

Kalaji, H.M., A. Jajoo, A. Oukarroum, M. Brestic and M. Zivcak, 2016. Chlorophyll a fluorescence as a tool to monitor physiological status of plants under abiotic stress conditions. *Acta Physiol. Plantarum*, 38: 102

Krause, G.H. and E. Weis, 1991. Chlorophyll fluorescence and photosynthesis: The basics. *Annu. Rev. Plant Physiol. Plant Mol. Biol*., 42: 313–349

Lee, H.Y., Y.N. Hong and W.S. Chow, 2001. Photoinactivation of photosystem II complexes and photoprotection by non-functional neighbours in *Capsicum annuum* L. leaves. *Planta*, 212: 332–342

Lichtenthaler, H.K. and A.R. Wellburn, 1983. Determinations of total carotenoids and chlorophylls a and b of leaf extracts in different solvents. *Biochem. Soc. Trans*., 603: 591–592

Lv, Y., C. Wang, Y. Jia, W. Wang, X. Ma, J. Du, G. Pu and X. Tian, 2014. Effects of sulfuric, nitric, and mixed acid rain on litter decomposition, soil microbial biomass, and enzyme activities in subtropical forests of China. *Appl. Soil Ecol*., 79: 1–9

Mai, B.R., Y.F. Zheng, J. Liang, X. Liu, L. Li and Y.C. Zhong, 2008. Effects of simulated acid rain on leaf photosynthate, growth, and yield of wheat. *Chin. J. Appl. Ecol*., 19: 2227–2233

Mcgegor, F., L. Ferreira and L. Morawska, 2003. New fluorescence parameters for monitoring photosynthesis in plants. *Photosynth. Res*., 78: 17–33

Neves, N.R., M.A. Oliva, D.D.C. Centeno, A.C. Costa, R.F. Ribas and E.G. Pereira, 2009. Photosynthesis and oxidative stress in the restinga plant species *Eugenia uniflora* L. exposed to simulated acid rain and iron ore dust deposition: potential use in environmental risk assessment. *Sci. Tot. Environ*., 407: 3740–3745

Shan, Y., T. Izuta, M. Aoki and T. Totsuka, 1997. Effects of O_3 and soil acidification, alone and in combination, on growth, gas exchange rate and chlorophyll content of red pine seedlings. *Water Air Soil Pollut*., 97: 355–366

Shaukat, S.S. and M.A. Khan, 2008. Growth and physiological responses of tomato (*Lycopersicon esculentum* Mill.) to simulated acid rain. *Pak. J. Bot*., 40: 2427–2435

Sheng, M., M. Tang, H. Chen, B. Yang, F. Zhang and Y. Huang, 2008. Influence of arbuscular mycorrhizae on photosynthesis and water status of maize plants under salt stress. *Mycorrhiza*, 18: 287–296

Smith, W.H., 1990. *Air Pollution and Forests Interaction between Air Contaminants and Forest Ecosystems*, 2nd edition, p: 618. Springer-Verlag, Berlin, Germany

Solomonson, L.P and A.M. Spehar, 1977. Model for the regulation of nitrate assimilation. *Nature*, 265: 373–375

Strasser, B.J., 1997. Donor side capacity of photosystem II probed by chlorophyll a fluorescence transients. *Photosynth. Res*., 52: 147–155

Strasser, R.J., M. Tsimilli-Michael and A. Srivastava, 2004. Analysis of the chlorophyll a fluorescence transient. *In*: *Advances in Photosynthesis and Respiration*, pp: 321–362. Papageorgiou and G. Govindjee (eds.). Chlorophyll A Fluorescence: A Signature of Photosynthesis. Kluwer Academic Publishers, The Netherlands

Strasser, R.J., A. Srivastava and Govindjee, 1995. Polyphasic chlorophyll a fluorescence transient in plants and cyanobacteria. *Photochem. Photobiol*., 61: 32–42

Synkova, H., N. Wilhelmova, D. Hola, D. Haisel and Z. Sestak, 1998. Comparison of chlorophyll fluorescence kinetics and photochemical activities of isolated chloroplasts in genetic analysis of *Lycopersicon esculentum* Mill. hybrids. *Photosynthesis*, 34: 427–438

Tong, S. and L. Zhang, 2014. Differential sensitivity of growth and net photosynthetic rates in five tree species seedlings under simulated acid rain stress. *Pollut. J. Environ. Stud*., 23: 2259–2264

Tu, J., H. Wang, Z. Zhang, X. Jin and W. Li, 2005. Trends in chemical composition of precipitation in Nanjing, China, during 1992–2003. *Atmos. Res*., 73: 283–298

Verma, A., A. Tewari and A. Azami, 2010. An impact of simulated acid rain of different pH-levels on some major vegetable plants in India. *Rep. Opin*., 2: 38–40

Wang, Y., L.J. Li and Y. Liu, 2012. Characteristics of atmospheric NO_2 in the Beijing-Tianjin-Hebei region and the Yangtze River Delta analyzed by satellite and ground observations. *Environ. Sci*., 33: 3686–3692

Zhang, H.H., N. Xu, X. Sui, H.X. Zhong, Z.P. Yin, X. Li and G.Y. Sun, 2018. Photosystem II function response to drought stress in leaves of two alfalfa (*Medicago sativa*) varieties. *Intl. J. Agric. Biol*., 20: 1012–1020

Zhao, D., Y. Pan, S. Deng, H. Shang, F. Wang and R. Chen, 2010. Effects of simulated acid rain on physiological and ecological characteristics of *Camellia sasanqua*. *Sci. Agric. Sin*., 43: 3191–3198

Zivcak, M., M. Brestic, K. Olsovska and P. Slamka, 2008. Performance index as a sensitive indicator of water stress in *Triticum aestivum* L. *Plant Soil Environ.*, 119: 133–139

(Received 21 March 2018; Accept 18 September 2018)